Perturbative description of inclusive single hadron production at HERA

S. Albino
II. Institute for Theoretical Physics, University of Hamburg,
Luruper Chaussee 149, 22761 Hamburg, Germany

Abstract

Light charged hadron production data in the current fragmentation region at HERA are calculated using next-to-leading order perturbative calculations and fragmentation functions obtained from similar data from e^+e^- reactions. General good agreement is found at large photon virtuality Q^2 and intermediate momentum fraction x_p, consistent with fragmentation function universality. The description of the small x_p and Q^2 region is improved by incorporating hadron mass effects.

1 Introduction

Unpolarized quark fragmentation functions (FFs) for charge-sign unidentified light charged hadrons $h^\pm = \pi^\pm$, $K^\pm$ and $p/\overline{p}$ have been well constrained by data from $e^+e^- \to h^\pm + X$ using calculations at next-to-leading order (NLO) accuracy. Due to universality in the factorization theorem, such FFs can be used to calculate the similar measurements of $ep \to e + h^\pm + X$. This contribution summarizes the main results of [1] comparing ep reaction data in the current fragmentation region from the H1 [2] and ZEUS [3] collaborations at HERA with calculations using FFs extracted from e^+e^- reactions.

The kinematic degrees of freedom are chosen to be the centre-of-mass energy $\sqrt{s}$ of the initial state ep system, the magnitude of the hard photon's virtuality $Q^2 = -q^2$, the Bjorken scaling variable $x = Q^2/(2P \cdot q)$ and the scaled detected hadron momentum $x_p = 2p_h \cdot q/q^2$. The normalized cross section (with the s dependence omitted for brevity) takes the form

$$F^{\text{proton } h^\pm}(\text{cuts}, x_{pA}, x_{pB}) = \frac{\int_{\text{cuts}} dQ^2 dx \int_{x_{pA}}^{x_{pB}} dx_p \frac{d\sigma^{\text{proton } h^\pm}}{dx_p dx dQ^2}(x, x_p, Q^2)}{\int_{\text{cuts}} dQ^2 dx \frac{d\sigma^{\text{proton}}}{dx dQ^2}(x, Q^2)}, \tag{1}$$

where "cuts" refers to a specified region in the (x, Q^2) plane, and where $x_{pA(B)}$ is the lower (upper) edge of the x_p bin. The cross section and the kinematic variables are frame invariant, and are measured in the Breit frame, defined to be the frame where the photon energy vanishes. In this frame the target fragmentation region ($x_p < 0$) contains the proton remnants, while the struck parton fragments into the current fragmentation region ($x_p > 0$), and the latter process is equivalent to the fragmentation of a parton into an event hemisphere in e^+e^- reactions. The factorization theorem dictates that, at leading twist, the highly virtual photon undergoes hard scattering with a parton in the proton moving in the same direction and carrying away an energy / momentum fraction y. One of the partons produced in this scattering undergoes fragmentation to the observed hadron $h^\pm$ moving in the same direction and carrying away an energy / momentum fraction z. In other words, after the change of integration variables $z \to x_p/z$ and $y \to x/y$, the factorized cross section in the numerator of Eq. (1) takes the form

$$\begin{aligned} \frac{d\sigma^{\text{proton } h^\pm}}{dx_p dx dQ^2}(x, x_p, Q^2) = &\int_{x_p}^1 \frac{dz}{z} \int_x^1 \frac{dy}{y} \sum_{ij} \frac{d\sigma^{ij}}{dz dy dQ^2}\left(y, z, \frac{Q^2}{\mu^2}, a_s(\mu^2)\right) \\ &\times f_i^{\text{proton}}\left(\frac{x}{y}, \mu^2\right) D_j^{h^\pm}\left(\frac{x_p}{z}, \mu^2\right), \end{aligned} \tag{2}$$

where f_i^{proton} is the parton distribution function (PDF) of parton i in the proton, $D_j^{h^\pm}$ the FF of parton j to $h^\pm$, $d\sigma^{ij}$ the equivalent factorized partonic observable given to NLO in Ref. [4], μ the factorization / renormalization scale which distinguishes the soft from the hard subprocesses and $a_s(\mu^2) = \alpha_s(\mu)/(2\pi)$.

2 Comparisons with data

At leading order in a_s, eq. (1) becomes

$$F^{\text{proton}\ h^{\pm}}(\text{cuts}, x_{pA}, x_{pB}) = \frac{\int_{x_{pA}}^{x_{pB}} dx_p \sum_I e_{q_I}^2(Q^2) G_I(Q^2) x_p D_I^{h^{\pm}}(x_p, Q^2)}{\sum_J e_{q_J}^2(Q^2) G_J(Q^2)}, \tag{3}$$

where the parton labels I, J are restricted to (anti)quarks q_I only, which have electric charges e_{q_I}, and $G_I(Q^2) = \int_{\text{cuts}} dx\ x f_I^{\text{proton}}(x, Q^2)$. In the limit that the G_I become independent of I, the numerator of Eq. (3) is equal to the equivalent LO result for $e^+e^- \to h^{\pm} + X$, and therefore the two types of observables are distinguished only by the G_I. If this discrepancy is small, a good description of HERA data is expected using FFs obtained from fits to e^+e^- data, such as the AKK [5], Kretzer [6] and KKP [7] FF sets [1] if universality and fixed order (FO) perturbation theory are reliable. Calculations using these sets for the H1 data are shown in Fig. 1, using the CTEQ6M PDF set [9] and the CYCLOPS program [10] here and throughout this work, unless otherwise stated. The strong disagreement between the FF sets at large x_p most likely arises from large experimental errors on the FFs due to poor constraints from e^+e^- reaction data at large momentum fraction. At high Q^2, the calculation for all 3 FF sets agrees well with the data. Therefore, the disagreements at large and small x_p values found with the lower Q^2 data may be due to effects beyond the FO approach at leading twist. For example, resummation of soft gluon emission logarithms that become large at small and large x_p may be necessary to improve the calculation here. This is illustrated in Fig. 2 (left) by the effect of scale variation on the calculation, being largest at small and large x_p. The effect of the observed hadron's mass m_h is also important at small x_p for low Q^2 values. For non-zero hadron mass, one has to distinguish between momentum, energy, light cone momentum etc., which are all equal when the hadron mass is negligible. According to the factorization theorem, the "momentum" fraction z appearing in eq. (2) is the fraction of light cone momentum carried away from the fragmenting parton by the observed hadron in a frame in which the spatial momenta of the virtual photon and the detected hadron are parallel, and $x_p = \xi_p(1 - m_h^2/(Q^2\xi_p^2))$ should be replaced by the ratio of the hadron's to the virtual photon's light cone momentum, ξ_p. Using this approach [1], one finds that the experimentally measured quantity $d\sigma^{\text{proton}\ h^{\pm}}/dx_p dx dQ^2$ is related to the calculated

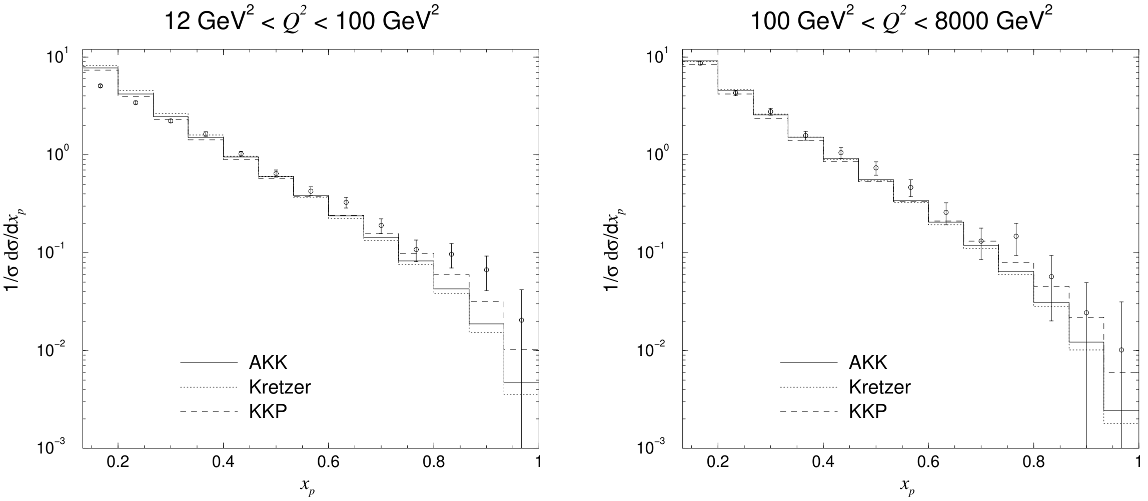

Fig. 1: Comparisons of theoretical predictions using the AKK, Kretzer and KKP FF sets with the x_p distributions from H1 [2].

---

[1] Since this work was completed, 3 further sets [8] have been extracted using improved theoretical and experimental input.

quantity $d\sigma^{\text{proton } h^{\pm}}/d\xi_p dx dQ^2$ by

$$\frac{d\sigma^{\text{proton } h^{\pm}}}{dx_p dx dQ^2}(x, x_p, Q^2) = \frac{1}{1 + \frac{m_h^2}{Q^2 \xi_p^2(x_p)}} \frac{d\sigma^{\text{proton } h^{\pm}}}{d\xi_p dx dQ^2}(x, \xi_p(x_p), Q^2), \tag{4}$$

which shows clearly that hadron mass effects become important at small x_p and low Q^2. According to Fig. 2, this correction improves the description in this region, if we compare the results of this figure with the low Q^2 results of Fig. 1. The choice $m_h = 0.5$ GeV represents an "average" mass for the light charged hadrons. We do not incorporate mass effects for the proton of the initial state, since this effect is expected to partially cancel between the numerator and denominator of eq. (1). By redoing the calculation with the MRST2001 PDF set [11], we see that the dependence on the choice of PDF set is small, particularly at small x_p, most likely because these quantities are well constrained but also because any variations in them are partially canceled between the numerator and denominator of eq. (1). As for e^+e^- reactions, the dependence on the gluon FF is small, particularly at large x_p.

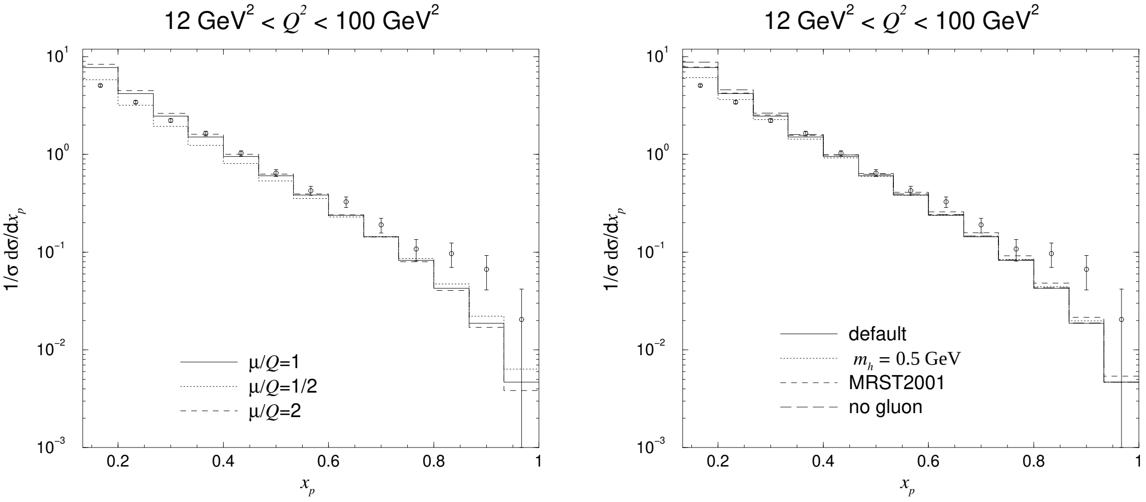

Fig. 2: As in Fig. 1, using only the AKK FF set. Left: The modifications arising from scale variation. Right: The modifications to the default predictions (solid line) arising from the replacement of the CTEQ6M PDF set by the MRST2001 PDF set of Ref. [11], from the removal of the evolved gluon, and from the incorporation of the hadron mass effect are shown.

To further verify these observations and inferences, we perform similar calculations for the ZEUS data. The different FF sets lead to similar results and good agreement with the data at large Q^2 and intermediate x_p (Fig. 3). The scale variation (Fig. 4, top) generally decreases with increasing Q^2, and is largest for small x_p. Both hadron mass effects and gluon fragmentation are most important at low Q^2 and small x_p (Fig. 4, bottom).

3 Conclusions

High Q^2 measurements of inclusive single hadron production at HERA are well described by perturbative QCD in the framework of the factorization theorem using available FF sets. Although some disagreement is found with data at lower Q^2, we note that there is significant room for improvement in the theory in this region, such as hadron mass effects studied in this work, but also resummation of the FO series at small and large x_p, higher twist effects and quark mass effects. Whether such effects are in fact relevant can be better verified by the effect of incorporating such data into global fits of FFs. More importantly, such data may also provide valuable information on the FFs' quark flavour components not constrained

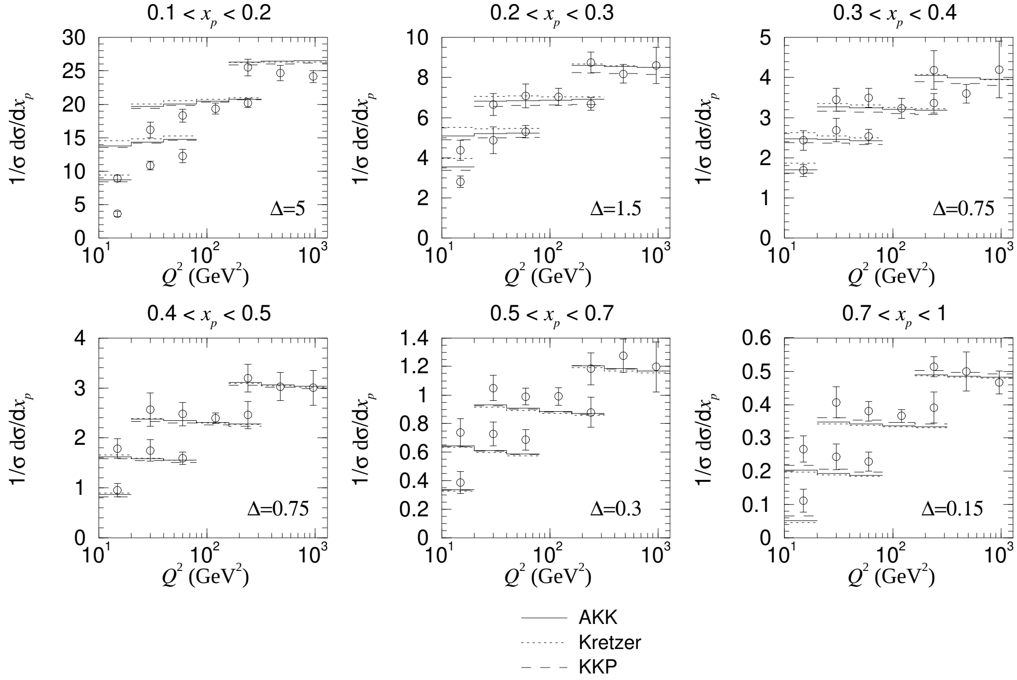

Fig. 3: As in Fig. 1, but for the ZEUS data [3]. Each data set is measured in a specific x_p-bin and, together with its predictions, is shifted upward relative to the one below by the indicated value for Δ.

by e^+e^- reaction data, particularly since these type of HERA measurements may now be made very precisely [12]. However, in order to constrain FFs for each hadron species individually, and to ensure that the data is not contaminated by light charged particles other than $\pi^\pm$, $K^\pm$ and $p/\overline{p}$, the hadron species of the HERA data need to be identified.

Acknowledgments

The author thanks Bernd A. Kniehl, Gustav Kramer and Carlos Sandoval for collaboration.

References

[1] S. Albino, B. A. Kniehl, G. Kramer and C. Sandoval, Phys. Rev. D **75**, 034018 (2007).

[2] C. Adloff *et al.* [H1 Collaboration], Nucl. Phys. B **504**, 3 (1997).

[3] J. Breitweg *et al.* [ZEUS Collaboration], Phys. Lett. B **414**, 428 (1997).

[4] G. Altarelli, R. K. Ellis, G. Martinelli, and S. Y. Pi, Nucl. Phys. B **160**, 301 (1979).

[5] S. Albino, B. A. Kniehl, and G. Kramer, Nucl. Phys. B **725**, 181 (2005).

[6] S. Kretzer, Phys. Rev. D **62**, 054001 (2000).

[7] B.A. Kniehl, G. Kramer, and B. Pötter, Nucl. Phys. B **582**, 514 (2000).

[8] M. Hirai, S. Kumano, T. H. Nagai and K. Sudoh, Phys. Rev. D 75 (2007) 094009; D. de Florian, R. Sassot and M. Stratmann Phys. Rev. D 75 114010 (2007); Phys. Rev. D 76 074033 (2007); S. Albino, B. A. Kniehl and G. Kramer, Nucl. Phys. B **803** (2008) 42.

[9] J. Pumplin, D. R. Stump, J. Huston, H. L. Lai, P. Nadolsky, and W. K. Tung, JHEP **0207**, 012 (2002).

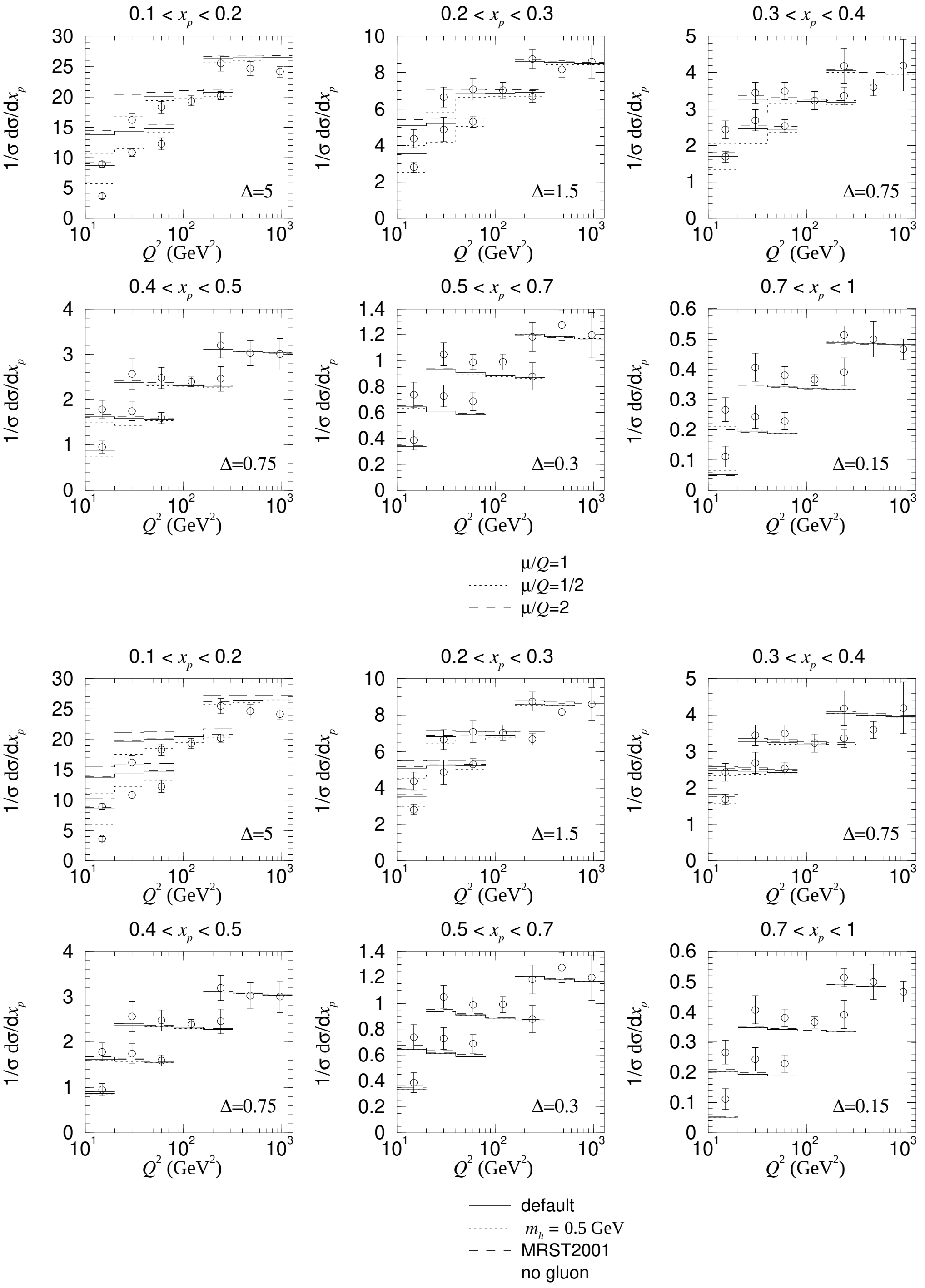

Fig. 4: As in Fig. 2, but for the ZEUS data [3].

[10] D. Graudenz, Fortsch. Phys. **45**, 629 (1997).

[11] A. D. Martin, R. G. Roberts, W. J. Stirling, and R. S. Thorne, Eur. Phys. J. C **23**, 73 (2002).

[12] F. D. Aaron *et al.* [H1 Collaboration], Phys. Lett. B **654**, 148 (2007); B. Brzozowska [ZEUS Collaboration], prepared for the 15th International Workshop on Deep-Inelastic Scattering and Related Subjects (DIS2007), Munich, Germany, April 2007.